Flexible Neural Electrode Arrays With Switch-Matrix Based on a Planar Silicon Process

Akifumi Fujishiro, Sou Takahashi, Kazuaki Sawada, Makoto Ishida, and Takeshi Kawano

Abstract—Herein, we fabricate a flexible microelectronic system using a conventional silicon (Si) integrated circuit process. The fabricated device is a <12-μm-thick film flexible 7 × 8 (56 ch) switch-matrix microelectrode array, which can be used to record the electrical activity from numerous three-dimensional biological tissues. The embedded Si-nMOSFETs/(111) in a polyimide flexible film exhibit a controlled threshed voltage with a leakage current of 10^{-11} A and a subthreshold swing of 123 mV/decade at a 50-mV drain voltage. The electrical characteristics between the flat and bent (with a 3-mm curvature radius) devices do not significantly change in a saline environment. These results indicate that the proposed method, which does not utilize conventional transfer printing technology, may be used to fabricate high-performance flexible electronics via a high-resolution lithography process. Such flexible electrode arrays may be applicable to high spatial-resolution recordings of neuronal signals from three-dimensional tissues, such as the brain surface, retina, and peripheral nerves.

Index Terms—Flexible electronics, MOSFETs, MEMS, neural electrode array, thin film transistors (TFTs).

I. INTRODUCTION

MICROELECTRODE arrays are powerful tools, which can record/stimulate neuronal cells in a tissue with a high spatiotemporal resolution [1]. Important characteristics of a minimally invasive electrode array for *in vivo* measurements [such as intracortical recording, Electrocorticogram (ECoG) recording and retinal implant] are flexibility [2], small size, and bio-compatibility [3]. To realize these requirements, microelectrode arrays based on flexible materials [4]–[6] and/or small packages of various modules (e.g., electrode arrays, signal processor, and RF circuit) [7] have been reported.

An early work to realize flexible electronics demonstrated the feasibility of transfer printing technology, facilitating the fabrication of flexible microelectrode arrays capable of recording signals from three-dimensional biological tissues [8]. The

great advantage of transfer printing in assembling MOSFETs on flexible substrates is that single crystal 'ribbons' of various high-mobility materials (e.g., Si, SiGe, and GaN) can be transferred [9], [10]. However, compared to the photolithography-based conventional silicon (Si) integrated circuit (IC) process, the disadvantage of the transfer-printing process is the insufficient alignment between small membranes and the substrate due to the assembly of micro/nanoscale membranes on the deformable target substrate (e.g., plastic films) [11].

To address processing issues, herein we propose a conventional Si IC–based flexible microelectronics process, which uses a silicon-on-insulator (SOI) substrate. By eliminating the transfer-printing process, the proposed method can be used to fabricate high-performance flexible electronics via high-resolution lithography patterning. To verify the feasibility of this process, we then fabricated <12 μm thick film flexible 7 × 8 (56 ch) switch-matrix microelectrode arrays, which can be used to record signals from three-dimensional biological tissues, such as the brain surface, retina, and peripheral nerves. Additionally, we demonstrate the electrical functionality of the fabricated flexible switch-matrix electrode arrays under bent and flat device conditions in saline solution.

II. FABRICATION

The proposed process consisted of two steps: i) a conventional planar Si IC process using a SOI substrate to fabricate Si-MOSFETs and ii) a post-MOS process to realize a flexible Si device [Fig. 1(a)]. In the first step, we fabricated the MOSFET/top Si of the SOI substrate using our in-house 10 μm gate length NMOSFET technology with 75 nm thick SiO_2 gate dielectrics (dry oxidation at 1000 °C for 60 min) and 350 nm thick heavily doped n-type poly-Si gate electrodes (low-pressure chemical vapor deposition at 625 °C for 60 min). Similar processes have been reported elsewhere [12], [13]. The SOI substrate consisted of a 2 μm thick (111)-top-Si (p-type with a resistivity of 3–20 Ω·cm)/1 μm thick BOX/525 μm thick (111)-Si substrate. Such a (111)-top Si may be applicable to assemble IC-compatible micro/nanoscale penetrating probe electrode arrays by vapor-liquid-solid growth of <111>-oriented Si micro/nanowires [14]. The threshold voltage of the NMOS devices were controlled by ion implantation into the channel region with BF_3 (3.5×10^{12} cm^{-2}, 65 keV). After the Si-MOSFET process, the passivation layer of SiO_2 over the source/drain electrode
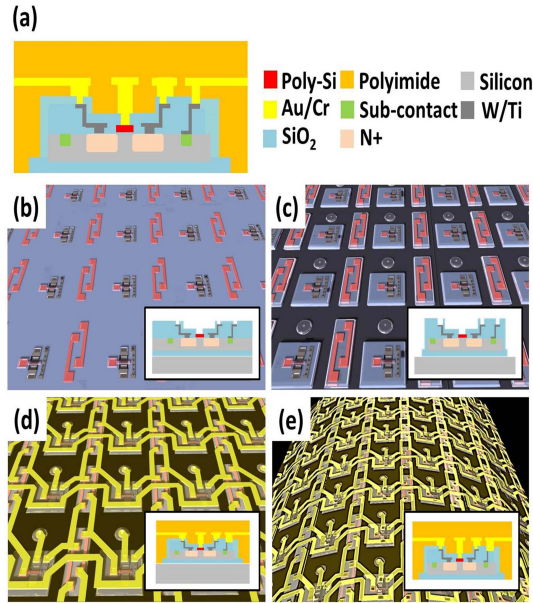
Fig. 1. Schematics of the fabrication sequence for a flexible device. (a) Cross-sectional image of the silicon-MOSFET embedded in a PI film. (b) Si-MOSFETs fabricated on a SOI substrate. (c) Si island formation by RIE. Black region in the top view represents the Si substrate. (d) Si islands covered by a flexible PI film. Device is metalized with Au/Cr. (e) Device is completed by removing the Si substrate.
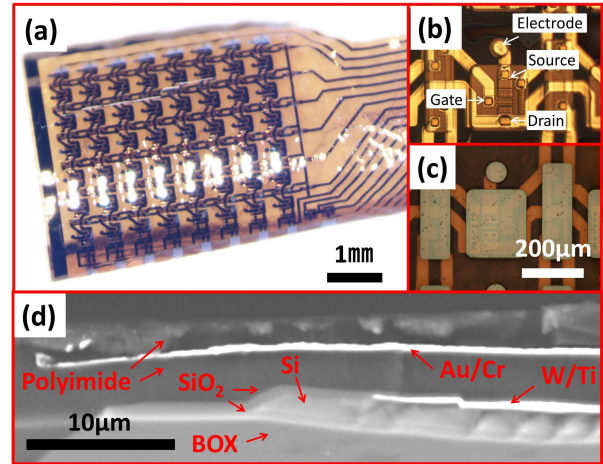

Fig. 2. Fabricated 7×8 (56 ch) flexible switch-matrix electrode array. (a) Photograph of the fabricated device. (b) Photograph of the front side of one unit cell consisting of a sensing Au electrode and a switching NMOSFET. (c) Photograph of the backside of the cell shown in (a). Poly-Si gate and source/drain electrodes can be observed due to the thin silicon island. (d) Cross-sectional SEM image of a silicon island embedded in a PI film with Au and W/Ti interconnections.

(W with adhesion Ti) and gate electrode regions was exposed for the subsequent flexible process [Fig. 1(b)].

Si islands were formed by photolithography patterning and reactive ion etching (RIE) with SF_6 gas [Fig. 1(c)]. Then a 500 nm thick SiO_2 layer [plasma enhanced chemical vapor deposition (PECVD)] was deposited to form the SiO_2 sidewall of the Si island. While a photoresist covered the SiO_2-encapsulated Si islands, the excess SiO_2 and the BOX layers without Si-island regions [black region in Fig. 1(c)] were simultaneously removed by a buffered hydrofluoric acid etch.

For the flexible substrate, we used a photosensitive poly-imide (PI) resist (PW-1270 of TORAY Inc). A 5 μm thick PI resist was formed over the sample by spin-coating [Fig. 1(d)]. The PI resist layer was subsequently patterned by photolitho-graphy to expose the contact holes of the island. The curing temperature of the PI resist was 340 °C for 1 h with N_2. For the interconnections between the islands, sputtering and lift-off were used to metallize multiple layers of Au/Cr (thicknesses = 300/20 nm). To encapsulate the device, except for the sensing electrodes (Au) and bonding pads, a second PI resist was coated over the interconnections using the same process [Fig. 1(d)]. Finally, the Si substrate was etched away with XeF_2 gas, while the BOX layer underneath the Si-island served as the etch-stopper [Fig. 1(e)].

III. RESULTS AND DISCUSSION

Fig. 2(a) shows a fabricated 7×8 (56 ch) switch-matrix electrode array where each sensing cell consists of a sensing Au electrode, a switching NMOSFET, and interconnection terminal islands [Fig. 2(b)]. The electrodes have diameters and spacings of 10 μm and 400 μm, respectively, because

this configuration will enable future recording applications of biological signals with a high spatial resolution [15]. The 183 Si-islands of a typical fabricated device (islands for sensing electrode, switching NMOSFET, and interconnection terminal) are formed without cracking or eroding the top-Si, resulting in a 100% device yield [Fig. 2(c)]. A cross-sectional observation of the fabricated device indicates that the PI/Si-island and only PI have total thicknesses of 11.3 μm and 9.8 μm, respectively [Fig. 2(d)].

To evaluate the electrical characteristics of the fabricated NMOSFETs/(111)-Si embedded in the PI film, we measured the drain current I_{DS}–gate voltage V_{GS} curves after removing the Si substrate [Fig. 1(a)]. The fabricated NMOSFETs with channel lengths and widths of 9 μm and 51 μm, respec-tively, exhibit a leakage current of less than 1.7×10^{-11} A, a threshold voltage of 0.2 V with a subthreshold swing of 123 mV/decade and an effective mobility of 558 cm^2/Vs in the linear region (drain voltage $V_{DS} =$ 50 mV) [Figs. 3(a) and (b)]. The on/off ratio is $>10^6$. Figure 3(a) also includes the electrical characteristics of the same NMOSFET prior to removing the Si substrate [Fig. 1(d)]. The changes in the leakage current, subthreshold swing and effective mobility are insignificant between the two MOSFETs, except for the threshold voltage (0.3 V). The effective mobility changed to 582 cm^2/Vs, while the device was bent outward [Fig. 1(e)] with a bending curvature radius of 5 mm. These results confirm that conventional planar IC–processed Si-MOSFETs can realize high-performance flexible electronics.

To verify the electrode functionality of the switch-matrix arrays and a device application for biological potential recordings, we measured the electrolyte-electrode interfacial impedance of the 10 μm diameter Au-electrode with and without device bending in saline solution (0.9% NaCl at room temperature) [Fig. 3(c)]. The radius of the inwardly bent device is 3 mm, which has a curvature applicable to numerous
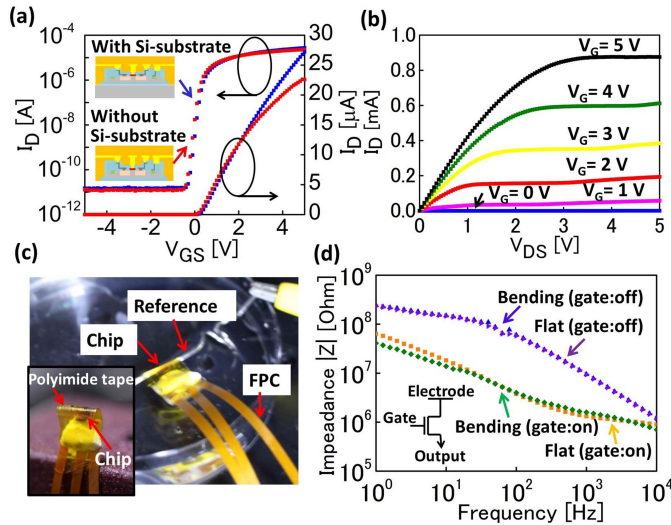
Fig. 3. Electrical characterizations of the fabricated device. (a) Drain current I_{DS}–gate voltage V_{GS} curves of a fabricated Si-NMOSFET/(111) (drain voltage $V_{DS} = 50$ mV) with and without the Si substrate. (b) Drain current I_{DS}–drain voltage V_{DS} characteristic of the device without the Si substrate shown in (a). (c) Electrical functionality of the device measured in saline. (d) Impedance of the Au electrode in a device immersed in saline under bent and flat device conditions. Radius of curvature of the bent device is 3 mm.

biological tissues (e.g., brain surface, retina and peripheral nerves). It should be noted that taping with a polyimide film electrically isolated the backside of the measured device.

Fig. 3(d) shows the magnitude of the impedance for a typical Au electrode measured in saline solution. In the off-state of the NMOSFET, the impedances of the Au electrode in the bent and flat devices are 9.40 MΩ and 9.41 MΩ at 1 kHz, respectively. In the on-state of the NMOSFET, the electrode impedances of the bent and flat devices are 1.59 MΩ and 1.31 MΩ at 1 kHz, respectively. These observations confirm that the electrical characteristics between the bent and flat devices do not significantly change in a saline environment. Without series NMOSFETs, an Au electrode with the same diameter exhibited similar impedance value of 1.87 MΩ at 1 kHz. As we previously reported [14], a high electrode impedance and embedded parasitic capacitances attenuate detected neuronal activities. According to this report, the fabricated device with a <2 MΩ electrode impedance has the recording capability with the input/output signal ratio of more than 57% at ~1 kHz. The recording input/output ratio can further be increased by reducing the electrode impedance such as the use of a larger diameter Au electrode (>10 μm) or a low impedance electrode material including Pt, PtO and IrO.

IV. CONCLUSION

We fabricated a flexible 7 × 8 (56ch) switch-matrix neural electrode array utilizing a conventional planar Si IC process on a SOI substrate. The proposed process demonstrates that high-resolution lithography patterning can fabricate a thin flexible device without utilizing conventional transfer-printing technology. In addition, the flexible electrode arrays may be applicable for high spatial-resolution recordings of the biological potentials of numerous three-dimensional tissues.

REFERENCES

[1] G. Schalk and E. C. Leuthardt, "Brain-computer interfaces using electrocorticographic signals," *IEEE Rev. Biomed. Eng.*, vol. 4, no. 4, pp. 140–154, Apr. 2011.

[2] L. J. Fernandez, A. Altuna, M. Tijero, et al., "Study of functional viability of SU-8-based microneedles for neural applications," *J. Micromech. Microeng.*, vol. 19, no. 2, pp. 025007-1–025007-3, 2009.

[3] D. H. Szarowski, M. D. Andersen, S. Retterer, et al., "Brain responses to micro-machined silicon devices," *Brain Res.*, vol. 983, pp. 23–35, Sep. 2003.

[4] P. J. Rousche, D. S. Pellinen, D. P. Pivin, et al., "Flexible polyimide-based intracortical electrode arrays with bioactive capability," *IEEE Trans. Biomed. Eng.*, vol. 48, no. 3, pp. 361–371, Mar. 2001.

[5] B. Rubehn, C. Bosman, R. Oostenveld, et al., "A MEMS-based flexible multichannel ECoG-electrode array," *J. Neural Eng.*, vol. 6, no. 3, pp. 036003-1–036003-6, 2009.

[6] T. Schanze, L. Hesse, C. Lau, et al., "An optically powered single-channel stimulation implant as test system for chronic biocompatibility and biostability of miniaturized retinal vision prostheses," *IEEE Trans. Biomed. Eng.*, vol. 54, no. 6, pp. 983–992, Jun. 2007.

[7] G. E. Perlin and K. D. Wise, "An ultra compact integrated front end for wireless neural recording microsystems," *J. Microelectromech. Syst.*, vol. 19, no. 6, pp. 1409–1421, Dec. 2010.

[8] J. Viventi, D. H. Kim, L. Vigeland, et al., "Flexible, foldable, actively multiplexed, high-density electrode array for mapping brain activity in vivo," *Nat. Neurosci.*, vol. 14, no. 4, pp. 1599–1605, 2011.

[9] A. Carlson, A. M. Bowen, Y. Huang, et al., "Transfer printing techniques for materials assembly and micro/nanodevice fabrication," *Adv. Mater.*, vol. 24, no. 39, pp. 5284–5318, Oct. 2012.

[10] J. H. Ahn, H. S. Kim, K. J. Lee, et al., "Heterogeneous three-dimensional electronics by use of printed semiconductor nanomaterials," *Science*, vol. 314, no. 5806, pp. 1754–1757, Dec. 2006.

[11] L. Sun, G. Qin, J. H. Seo, et al., "12-GHz thin-film transistors on transferrable silicon nanomembranes for high performance flexible electronics," *Small*, vol. 6, no. 22, pp. 2553–2557, Nov. 2010.

[12] T. Kawano, Y. Kato, R. Tani, et al., "Selective vapor-liquid-solid epitaxial growth of micro-Si probe electrode arrays with on-chip MOSFETs on Si (111) substrates," *IEEE Trans. Electron Devices*, vol. 51, no. 3, pp. 415–420, Mar. 2004.

[13] A. Okugawa, K. Mayumi, A. Ikedo, et al., "Heterogeneously integrated vapor-liquid-solid grown silicon probes/(111) and silicon MOSFETs/(100)," *IEEE Electron Device Lett.*, vol. 32, no. 5, pp. 683–685, May 2011.

[14] A. Fujishiro, H. Kaneko, T. Kawashima, et al., "A penetrating micro-scale diameter probe array for in vivo neuron spike recordings," in *Proc. IEEE 24th Int. Conf. MEMS*, Jan. 2011, pp. 1011–1014.

[15] A. Ritaccio, D. Boatman-Reich, P. Brunner, et al., "Proceedings of the Second International Workshop on Advances in Electrocorticography," *Epilepsy Behavior*, vol. 22, no. 4, pp. 641–650, Dec. 2011.